

# Production of the bottomonium-like $Z_b$ states in $e-h$ and ultraperipheral $h-h$ collisions

Xiao-Yun Wang<sup>1,\*</sup>, Wei Kou<sup>2,3</sup>, Qing-Yong Lin<sup>4,†</sup>, Ya-Ping Xie<sup>2,3,‡</sup> and Xurong Chen<sup>2,3,5§</sup>

<sup>1</sup>*Department of physics, Lanzhou University of Technology, Lanzhou 730050, China*

<sup>2</sup>*Institute of Modern Physics, Chinese Academy of Sciences, Lanzhou 730000, China*

<sup>3</sup>*University of Chinese Academy of Sciences, Beijing 100049, China*

<sup>4</sup>*Department of Physics, Jimei University, Xiamen 361021, China*

<sup>5</sup>*Guangdong Provincial Key Laboratory of Nuclear Science, Institute of Quantum Matter, South China Normal University, Guangzhou 510006, China*

Alexey Guskov<sup>6¶</sup>

<sup>6</sup>*Joint Institute for Nuclear Research, Dubna 141980, Russia*

The photoproduction of bottomonium-like states  $Z_b(10610)$  and  $Z_b(10650)$  via  $\gamma p$  scattering is studied within an effective Lagrangian approach and the vector-meson-dominance model. The Regge model is employed to calculate the photoproduction of  $Z_b$  states via  $t$ -channel with  $\pi$  exchange. The numerical results show that the values of the total cross-sections of  $Z_b(10610)$  and  $Z_b(10650)$  can reach 0.09 nb and 0.02 nb, respectively, near the center of mass energy of 22 GeV. The experimental measurements and studies on the photoproduction of  $Z_b$  states near energy region around  $W \simeq 22$  GeV is suggested. Moreover, with the help of eSTARlight and STARlight programs, one obtains the cross-sections and event numbers of  $Z_b(10610)$  production in electron-ion collision (EIC) and Ultraperipheral collisions (UPCs). The results show that a considerable number of events from  $Z_b(10610)$  can be produced on the relevant experiments of EICs and UPCs. Also, one calculates the rates and kinematic distributions for  $\gamma p \rightarrow Z_b n$  in  $ep$  and  $pA$  collisions via EICs and UPCs, and the relevant results will provide an important reference for the RHIC, LHC, EIC-US, LHeC, and FCC experiments to search for the bottomonium-like  $Z_b$  states.

PACS numbers: 13.60.Le, 13.85.-t, 11.10.Ef, 12.40.Vv, 12.40.Nn

## I. INTRODUCTION

In recent decades, with the continuous progress of high energy physics experiments, more and more exotic hadron states have been discovered [1–3]. The study of the production and properties of exotic hadron states is not only conducive to the improvement and development of hadron spectrum and hadron classification, but also of great significance for an in-depth understanding of non-perturbative quantum chromodynamics (QCD). The candidate particles of the exotic states that have been discovered are mostly concentrated in the charm energy region, and the discovered exotic states in the bottom quark energy region are still very limited [1–3]. In 2011, two bottomonium-like states  $Z_b(10610)$  and  $Z_b(10650)$ , were observed by the Belle Collaboration [4], and a series of subsequent experiments also discovered these two states from different decay channels [4–7]. Since the quantum numbers and decay properties of  $Z_b(10610)$  and  $Z_b(10650)$  are very similar [1], for convenience,  $Z_b(10610)$  and  $Z_b(10650)$  will be abbreviated as  $Z_b$  later. These two states are considered to be different from the traditional hadron states and are likely to contain at least four quarks [2, 3].

Observations of the  $Z_b$  has inspired extensive studies on the underlying properties, where tetraquark state [8–11], hadronic molecule interpretation [12–17] are performed. More discussions can be found in Refs. [2, 18]. In Ref. [3], the authors pointed out that, since these two states are discovered through the decay reaction of the bottomonium, the contribution of the triangular singularities during the reaction cannot be neglected, which means that one cannot yet determine whether these two states are genuine particles. At present, investigating  $Z_b$  is still an interesting research topic.

Besides the analysis of the mass spectrum and the decay behavior, studying the production of  $Z_b$  in more different mechanisms is very helpful to obtain definite evidence for their nature as genuine states. As well known, the meson photoproduction process was proposed to be an effective way to search for exotic states [19–27]. We take notice of the  $Z_b \rightarrow \Upsilon(nS)\pi^+$  decay modes, which indicates that there exists a strong coupling between  $Z_b$  and  $\Upsilon(nS)\pi^+$ . Since  $\Upsilon(nS)$  is a vector meson, we suppose that we can carry out the production of the  $Z_b$  states through the meson photoproduction. In the current work, the photoproduction of

---

\*xywang@lut.edu.cn (Corresponding author)

†qylin@jmu.edu.cn

‡xieyaping@impcas.ac.cn

§xchen@impcas.ac.cn

¶avg@jinr.ru

$Z_b$  will be studied within the framework of the effective Lagrangian approach and the vector-meson-dominance (VMD) model [28–30]. The calculations will provide crucial information on the suitable process and the best energy window of searching for the  $Z_b$  states on related photoproduction experiments.

In hadron-hadron collisions, when the impact parameter between the two nuclei is larger than the sum of radii of two nuclei, the direct strong interaction between the nuclei is suppressed since the strong interaction is short range. However, the electromagnetic interaction can not be neglected since it is long-range interaction. This collision is denoted as ultraperipheral collisions (UPCs) [31, 32]. In UPCs, the photon is almost a real photon when the mass number of an atomic nucleus is larger than 16. Hence, UPCs is a good platform to study photoproduction with small photon virtuality.

Electron-ions collider (EIC) is an important platform to investigate nucleon structure in the future. In EICs, the electron scatters off a nucleon or nuclei via a virtual photon. Then, vector mesons and exotic states can be produced. Thus, the photoproduction of exotic states can be studied in EICs in the future. There are a couple of proposed EICs plans in the world, for example, EicC, EIC-US, LHeC and FCC are proposed [33–36]. In EICs, the photon emitted from the electron beam has large virtuality. This is different from the photon in UPCs. Hence, EICs can be applied to investigate the photoproduction in a large  $Q^2$  region.

STARlight and eSTARlight are two important Monte-Carlo packages to simulate the photoproduction of vector mesons and exotic states in UPCs and EICs [37, 38, 42]. The cross-sections of vector mesons and exotic states produced in photon-proton scattering is needed in the simulation process. The information of four-momentum of final states are produced in the simulation processes. At the same, the total cross sections of vector mesons or exotic states in UPCs and EICs are performed in STARlight and eSTARlight. In this work, the total cross sections of  $Z_b$  at UPCs and proposed EICs will be performed adopting STARlight and eSTARlight packages. The rapidity and transverse momentum distributions of  $Z_b$  will be presented. These distributions will be useful for the detector systems in future experiments.

This paper is organized as follows. After the introduction, one presents the formalism for the production of  $Z_b$  in Section II. The numerical results of the  $Z_b$  production follow in Section III. Finally, the paper ends with a summary.

## II. FORMALISM

### A. $Z_b$ photoproduction in $\gamma p \rightarrow Z_b n$ reaction

In this work, the production of the hidden-bottom  $Z_b(10610)$  and  $Z_b(10650)$  states via  $\gamma p \rightarrow Z_b n$  reaction will be studied with an effective Lagrangian approach. In the PDG book [1], one finds that the  $Z_b(10610)$  or  $Z_b(10650)$  can decay to a bottomonium plus  $\pi$  meson with a branching ratio of a few percent. Since  $Z_b$  states are not directly coupled to photons, the VMD model can be used to calculate the photoproduction of  $Z_b$  states through the  $t$  channel with  $\pi$  exchange. The Feynman diagram of the  $\gamma p \rightarrow Z_b n$  reaction via  $t$  channel  $\pi$  exchange is depicted in Fig. 1. It is noted from Fig. 1 that we only consider the coupling of  $\Upsilon(1s, 2s, 3s)$  and photons. Also, although  $Z_b$  can also decay to  $h_b(1p, 2p)\pi$ , since the parity of the  $h_b$  state is opposite to that of the photon, the direct coupling of  $h_b$  to photon can be neglected.

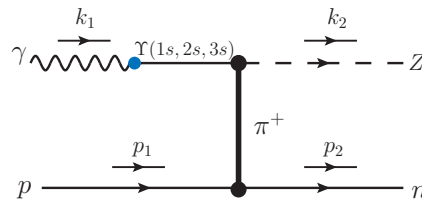


FIG. 1: Feynman diagrams for the reaction  $\gamma p \rightarrow Z_b n$ .

#### 1. Lagrangians for the $Z_b$ production

In PDG [1], the spin-parity quantum numbers of  $Z_b(10610)$  and  $Z_b(10650)$  are both  $1^+$ , thus the Lagrangian densities for the vertices of  $Z_b \Upsilon \pi$  and  $\pi NN$  are written as [19, 40],

$$\mathcal{L}_{Z_b \Upsilon \pi} = \frac{g_{Z_b \Upsilon \pi}}{M_{Z_b}} (\partial^\mu \Upsilon^\nu \partial_\mu \pi Z_{b\nu} - \partial^\mu \Upsilon^\nu \partial_\nu \pi Z_{b\mu}), \quad (1)$$

$$\mathcal{L}_{\pi NN} = -i g_{\pi NN} \bar{N} \gamma_5 \vec{\tau} \cdot \vec{\pi} N, \quad (2)$$

where  $Z_b$ ,  $\Upsilon$ ,  $\pi$  and  $N$  denote the fields of  $Z_b(10610)/Z_b(10650)$ ,  $\Upsilon$ , pion and nucleon meson, respectively. Here, the  $g_{\pi NN}^2/4\pi = 12.96$  is adopted [41].

The coupling constant  $g_{Z_b\Upsilon\pi}$  can be derived from the corresponding decay width

$$\Gamma_{Z_b \rightarrow \Upsilon\pi} = \left( \frac{g_{Z_b\Upsilon\pi}}{M_{Z_b}} \right)^2 \frac{|\vec{p}_\pi^{\text{c.m.}}|^2}{24\pi M_{Z_b}^2} \times \left[ \frac{(M_{Z_b}^2 - m_\Upsilon^2 - m_\pi^2)^2}{2} + m_\Upsilon^2 E_\pi^2 \right], \quad (3)$$

with

$$|\vec{p}_\pi^{\text{c.m.}}| = \frac{\lambda^{1/2}(M_{Z_b}^2, m_\Upsilon^2, m_\pi^2)}{2M_{Z_b}}, \quad (4)$$

$$E_\pi = \sqrt{|\vec{p}_\pi^{\text{c.m.}}|^2 + m_\pi^2}, \quad (5)$$

where  $\lambda$  is the Källén function with  $\lambda(x, y, z) \equiv \sqrt{(x - y - z)^2 - 4yz}$ , and  $M_{Z_b}$ ,  $m_\Upsilon$ , and  $m_\pi$  are the masses of  $Z_b$ ,  $\Upsilon$ , and pion meson, respectively. The partial decay widths and coupling constants for  $Z_b \rightarrow \Upsilon\pi$  are listed in Table I.

TABLE I: The values of coupling constants  $g_{Z_b\Upsilon\pi}$  by taking the corresponding decay width of  $\Gamma_{Z_b \rightarrow \Upsilon\pi}$  in PDG book [1]. Here the unit of width is MeV.

states	$\Gamma_{Z_b \rightarrow \Upsilon(1S)\pi}$	$g_{Z_b\Upsilon(1S)\pi}$	$\Gamma_{Z_b \rightarrow \Upsilon(2S)\pi}$	$g_{Z_b\Upsilon(2S)\pi}$	$\Gamma_{Z_b \rightarrow \Upsilon(3S)\pi}$	$g_{Z_b\Upsilon(3S)\pi}$
$Z_b(10610)$	0.099	0.487	0.662	3.299	0.386	9.292
$Z_b(10650)$	0.019	0.206	0.161	1.468	0.184	4.916

The coupling of  $Z_b$  to the photon can be derived under the VMD mechanism [28–30]. In the VMD mechanism, a real photon can fluctuate into a virtual vector meson, which subsequently scatters off the target proton.

The Lagrangian depicting the coupling of the meson  $\Upsilon$  with a photon reads as [24, 25]

$$\mathcal{L}_{\Upsilon\gamma} = -\frac{em_\Upsilon^2}{f_\Upsilon} \Upsilon_\mu A^\mu, \quad (6)$$

where  $f_\Upsilon$  is the  $\Upsilon$  decay constant. Thus one gets the expression for the  $\Upsilon \rightarrow e^+e^-$  decay width,

$$\Gamma_{\Upsilon \rightarrow e^+e^-} = \left( \frac{e}{f_\Upsilon} \right)^2 \frac{8\alpha |\vec{p}_e^{\text{c.m.}}|^3}{3m_\Upsilon^2}, \quad (7)$$

where  $\vec{p}_e^{\text{c.m.}}$  denotes the three-momentum of an electron in the rest frame of the  $\Upsilon$  meson.  $\alpha = e^2/4\pi = 1/137$  is the electromagnetic fine structure constant. With the partial decay width of  $\Upsilon(1s, 2s, 3s) \rightarrow e^+e^-$  [1], one gets  $e/f_{\Upsilon(1s)} \simeq 0.008$ ,  $e/f_{\Upsilon(2s)} \simeq 0.005$  and  $e/f_{\Upsilon(3s)} \simeq 0.004$ .

## 2. Reggeized $t$ channel

Since the energy corresponding to the  $\gamma p \rightarrow Z_b n$  reaction is above 10 GeV, the Reggeized treatment will be applied to the  $t$  channel process. Usually, one just needs to replace the Feynman propagator with the Regge propagator as

$$\frac{1}{t - m_\pi^2} \rightarrow \left( \frac{s}{s_{scale}} \right)^{\alpha_\pi(t)} \frac{\pi\alpha'_\pi}{\Gamma[1 + \alpha_\pi(t)] \sin[\pi\alpha_\pi(t)]}, \quad (8)$$

where the scale factor  $s_{scale}$  is fixed at 1 GeV. In addition, the Regge trajectories of  $\alpha_\pi(t)$  is written as [40],

$$\alpha_\pi(t) = 0.7(t - m_\pi^2). \quad (9)$$

It can be seen that no free parameters have been added after introducing the Regge model.

### 3. Amplitude

Based on the Lagrangians above, the scattering amplitude for the reaction  $\gamma p \rightarrow Z_b n$  can be constructed as

$$-i\mathcal{M}_{\gamma p \rightarrow Z_b n} = \epsilon_{Z_b}^\mu(k_2)\bar{u}(p_2)\mathcal{A}_{\mu\nu}u(p_1)\epsilon_\nu^\gamma(k_1), \quad (10)$$

where  $u$  is the Dirac spinor of nucleon, and  $\epsilon_{Z_b}$  and  $\epsilon_\gamma$  are the polarization vectors of  $Z_b$  meson and photon, respectively. The reduced amplitude  $\mathcal{A}_{\mu\nu}$  for the  $t$  channel  $Z_b$  photoproduction reads

$$\begin{aligned} \mathcal{A}_{\mu\nu} = & -i(\sqrt{2}g_{\pi NN}\frac{g_{Z_b\gamma\pi}}{M_{Z_b}}\frac{e}{f_\pi})\gamma_5[k_1 \cdot (k_2 - k_1)g_{\mu\nu} - k_{1\mu}(k_2 - k_1)_\nu] \\ & \times \frac{1}{q^2 - m_\pi^2}\mathcal{F}_{\pi NN}(q^2)\mathcal{F}_{Z_b\gamma\pi}(q^2), \end{aligned} \quad (11)$$

For the  $t$ -channel meson exchanges [19, 20, 23, 40], the general form factor  $\mathcal{F}_i(q_i^2)$  consisting of  $\mathcal{F}_{Z_b\gamma\pi} = (m_\pi^2 - m_{Z_b}^2)/(m_\pi^2 - q_i^2)$  and  $\mathcal{F}_{\pi NN} = (\Lambda_t^2 - m_\pi^2)/(\Lambda_t^2 - q_i^2)$  are taken into account. Here,  $q_i$  and  $m_\pi$  are 4-momentum and mass of the  $\pi$  meson, respectively. The cutoff  $\Lambda_t$  will be taken as 0.7 GeV, which is the same as that in Ref. [19, 21–23].

With the preparation in the previous sections, the differential cross section in the center of mass (c.m.) frame is written as

$$\frac{d\sigma}{d\cos\theta} = \frac{1}{32\pi s} \frac{|\vec{k}_2^{\text{c.m.}}|}{|\vec{k}_1^{\text{c.m.}}|} \left( \frac{1}{4} \sum_\lambda |\mathcal{M}|^2 \right), \quad (12)$$

Here,  $s = (k_1 + p_1)^2$ , and  $\theta$  denotes the angle of the outgoing  $Z_b$  meson relative to  $\gamma$  beam direction in the c.m. frame.  $\vec{k}_1^{\text{c.m.}}$  and  $\vec{k}_2^{\text{c.m.}}$  are the three-momenta of the initial photon beam and final  $Z_b$  meson, respectively.

### B. $Z_b$ production in EIC and UPCs

In the electron-proton scattering, the cross section of  $Z_b$  is given by [38, 42]

$$\sigma(ep \rightarrow eZ_b n) = \int dk dQ^2 \frac{dN^2(k, Q^2)}{dk dQ^2} \sigma_{\gamma^* p \rightarrow Z_b n}(W, Q^2), \quad (13)$$

where  $k$  is the momentum of the photon emitted from electron in target rest frame,  $W$  is the c.m. energy of the photon and proton system, and  $Q^2$  is the virtuality of the photon. The photon flux reads as [43]

$$\frac{d^2N(k, Q^2)}{dk dQ^2} = \frac{\alpha}{\pi k Q^2} \left[ 1 - \frac{k}{E_e} + \frac{k^2}{2E_e^2} - \left( 1 - \frac{k}{E_e} \right) \left| \frac{Q_{\min}^2}{Q^2} \right| \right]. \quad (14)$$

The  $Q^2$  dependence of  $\sigma_{\gamma^* p \rightarrow Z_b n}(W, Q^2)$  is factorized as

$$\sigma_{\gamma^* p \rightarrow Z_b n}(W, Q^2) = \sigma_{\gamma p \rightarrow Z_b n}(W, Q^2 = 0) \left( \frac{M_V^2}{M_V^2 + Q^2} \right)^\eta, \quad (15)$$

where  $M_V$  is mass of the vector meson. Since there is no parameter for  $Z_b$  state, we apply the same  $\eta$  from  $J/\psi$  as Ref. [38]. This assumption has very little impact on the project for  $Z_b$  because we consider the  $0 < Q^2 < 1\text{GeV}^2$ , which is quasi-real events[44].

The cross-section of an exotic charged particle in UPCs is computed in integrating the photon flux and photon-proton cross-section. The photon flux represents the number as a function momentum of the photon emitted from a nucleus. In  $p$ - $A$  UPCs, the cross section of the  $pA \rightarrow nAZ_b$  reads [37]

$$\sigma(pA \rightarrow AZ_b n) = \int dk \frac{dN_\gamma(k)}{dk} \sigma_{\gamma p \rightarrow Z_b n}(W). \quad (16)$$

where  $k$  is the momentum of the real photon emitted from nucleus,  $W$  is the c.m. energy of the photon and proton system. The photon flux of the photon emitted from nucleus is given as [45]

$$\frac{dN_\gamma(k)}{dk} = \frac{2Z^2\alpha}{\pi k} (XK_0(X)K_1(X) - \frac{X^2}{2}[K_1^2(X) - K_0^2(X)]). \quad (17)$$

where  $X = b_{min}k/\gamma_L$ ,  $b_{min} = R_A + R_p$  is sum of radii of proton and nucleus.  $\gamma_L = \sqrt{s}/2m_p$  is the Lorentz boost factor.  $K_0(x)$  and  $K_1(x)$  are the modified Bessel functions.  $Z$  denotes the charge number of the nucleus.

Adopting the cross-sections of  $Z_b$  in photon-proton interaction, we can obtain the  $Z_b$  cross-sections in  $e-p$  scattering in EIC and  $p-A$  UPCs. With the help of eSTARlight and STARlight packages, we can simulate the  $Z_b$  production processes and get the four-momentum of final states. Then, we will further obtain the  $Z_b$  in rapidity distributions and transverse momentum distributions, where the rapidity is defined as  $y = \frac{1}{2} \ln[(E + p_z)/(E - p_z)]$ .

### III. NUMERICAL RESULTS

#### A. Photoproduction of $Z_b$

In Fig. 2 we present the total cross sections for the reaction  $\gamma p \rightarrow Z_b n$  from threshold to 50 GeV of the c.m. energy. One finds that the total cross-section of the  $\gamma p \rightarrow Z_b(10610)n$  scattering process reaches a maximum at the center of mass energy  $W \simeq 22$  GeV, which is about 0.09 nb. Also, one notice that when the cutoff parameter is changed from 0.5 to 0.9 GeV, the total cross section of the  $\gamma p \rightarrow Z_b(10610)n$  at  $W \simeq 22$  GeV is approximately between 0.06 and 0.12 nb.

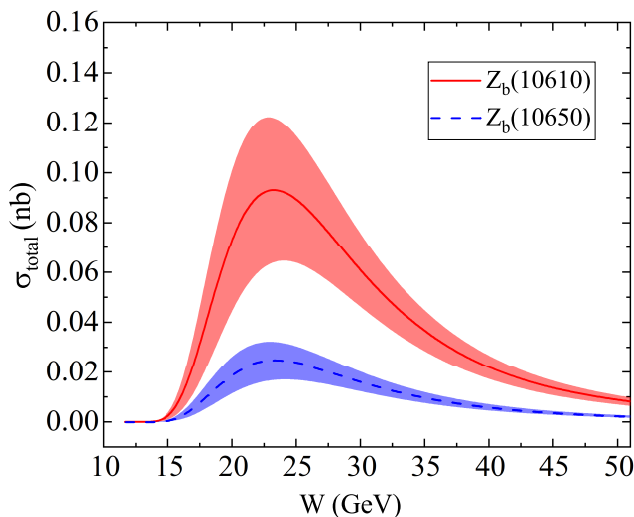


FIG. 2: The total cross section for the  $\gamma p \rightarrow Z_b n$  reaction via pionic Regge trajectory exchange. The red solid, and blue dashed lines are for the  $Z_b(10610)$ , and the  $Z_b(10650)$ , respectively. Here, the value of cutoff  $\Lambda_t$  is taken as  $0.7 \pm 0.2$  GeV. The bands stand for the error bar of the cutoff  $\Lambda_t$ .

#### B. $Z_b$ production in EIC and UPCs

Photoproduction measurement is an important test of the structure of exotic states. Since the energy span of EICs and UPCs facilities is large, it is advantageous to find the exotic states in the bottom quark energy region. Based on the previous  $Z_b$  photoproduction results, with the help of eSTARlight and STARlight programs, one obtains the cross-sections and event numbers of  $Z_b(10610)$  production in EICs and UPCs. As presented in Tab II, the results based on the several accelerator devices are calculated. The cross-section of  $Z_b(10610)$  in UPCs is larger than that in EICs since the photon flux of the nucleus is larger than the electron beam. However, the event number of  $Z_b(10610)$  in EICs is larger than that in UPCs, especially FCC.

It can be seen from Tab. II that the differences between the total cross sections in EICs are small since the cross-section of EICs is not very sensitive to the collide energies. However, the cross-section of  $Z_b$  in EICs heavily depends on the value of the cross-sections of  $Z_b$  photoproduction. It can be seen from Fig. 2 that if the c.m. energy is too small, the photoproduced cross-sections of  $Z_b$  will also be small, which indirectly leads to small cross-sections of  $Z_b$  in EICs. For the situation of EicC [33], the present designation of colliding energies of EicC is 5 GeV vs 20 GeV, therefore, the c.m energy is about 16.7 GeV. Thus the cross-sections of  $Z_b(10610)$  in EicC will be very small. Tab. III shows the cross-section of  $Z_b$  in EicC and the number of the event when the beam energy is up to 10 GeV vs 100 GeV. The relevant results will provide theoretical references for future experimental measurements and upgrades.

TABLE II: Cross sections and event numbers of  $Z_b(10610)$  in  $e-p$  scattering and  $p-A$  UPCs. The integrated luminosities are the same as Ref.[42]. The luminosity  $15 \times 10^{33} \text{ cm}^{-2} \text{ s}^{-1}$  was assumed for  $10^7$  s of running was assumed for FCC [36].

	$e-p$ EIC-US	$e-p$ LHeC	$e-p$ FCC	$p-Au$ RHIC	$p-Pb$ LHC
Beam energy, GeV	18 (e) vs. 275 (p)	60 (e) vs. $7 \times 10^3$ (p)	60 (e) vs. $50 \times 10^3$ (p)	100 (p) vs. 100 (Au)	$7 \times 10^3$ (p) vs. $2.778 \times 10^3$ (Pb)
Integrated luminosity	$10 \text{ fb}^{-1}$	$10 \text{ fb}^{-1}$	$150 \text{ fb}^{-1}$	$4.5 \text{ pb}^{-1}$	$2 \text{ pb}^{-1}$
$Z_b(10610)$ Cross sections	6.2 pb	8.5 pb	9.8 pb	2.0 nb	30 nb
Expected statistics, $10^6$ events	0.062	0.085	1.5	0.0090	0.060

TABLE III: Cross sections and event numbers of  $Z_b(10610)$  in  $e-p$  collision. Here, the integrated luminosity is taken as  $10 \text{ fb}^{-1}$ , which is the current design value of EicC [33]

Beam energy	5 (e) vs. 20 (p)	5 (e) vs. 30 (p)	10 (e) vs. 50 (p)	10 (e) vs. 100 (p)
$Z_b(10610)$ cross sections	0.52 pb	1.3 pb	3.4 pb	4.4 pb
Expected statistics, $10^3$ events	5.2	13	34	44

For the  $Z_b(10610)$  production in EICs and UPCs processes, we also present the rapidity distributions of  $Z_b(10610)$  in  $e-p$  and  $p-A$  processes, as shown in Fig. 3. These two distributions are relatively wide, which are related to the production mechanism of  $Z_b$  through  $t$ -channel with pionic Regge trajectory exchange [23]. This indicates that the distribution shape of the rapidity and transverse momentum reflects the shape of the cross-section in Fig. 2. From the left graph in Fig. 3, it can be seen that photoproduction of EIC-US is near mid-rapidity and it is easy to identify in the detector system. From the right graph of Fig. 3, we can also conclude that it is easy to observe  $Z_b(10610)$  in  $p-Au$  UPCs than  $p-Pb$  UPCs since the  $Z_b(10610)$  will be produced near mid-rapidity.

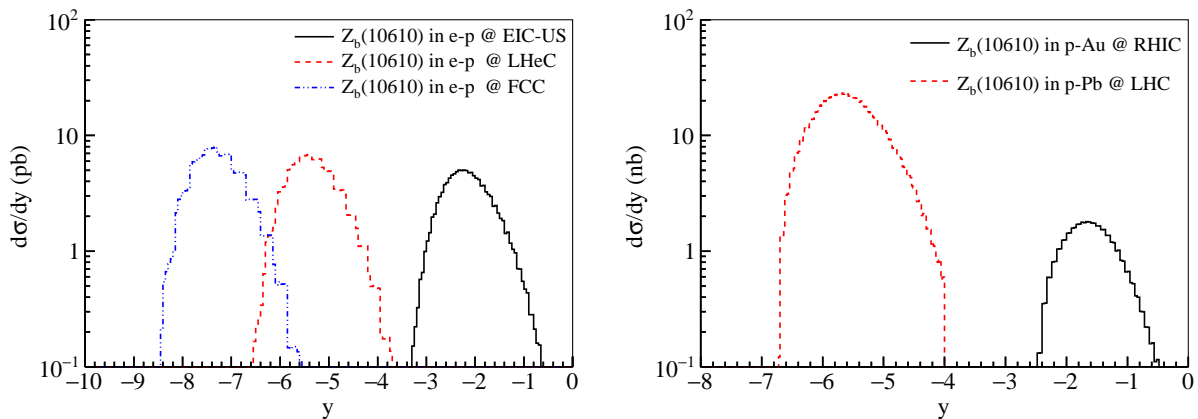


FIG. 3: (Color online) Rapidity distributions of  $Z_b(10610)$  in  $e-p$  at EIC-US, LHeC and FCC with  $0 < Q^2 < 1 \text{ GeV}^2$  and  $p-Au$  and  $p-Pb$  UPCs at RHIC and LHC.

In addition, the transverse momentum distributions in  $e-p$  scattering and  $p-A$  UPCs are also shown in Fig. 4. These results can be used as predictions for experiments. We notice that the three transverse momenta of EICs are closed to each other since the total cross-sections are closed to each other. These distributions can be employed to identifying the exotic states. In  $p-A$  UPCs, the difference between the two distributions is large because the total cross-section in  $p-Pb$  is larger than the cross-section in  $p-Au$ . It can be founded that the largest value of transverse momentum is about 0.2 - 0.4 GeV in both EICs and UPCs.

Moreover, We also give the  $t$ -distribution for the  $Z_b(10610)$  production in  $e-p$  and  $p-A$  UPCs in Fig. 5. The  $t$ -distributions are close to each other in three EICs and are different in two UPCs. These conclusions are the same as the transverse momentum distributions. Due to the adoption of the Regge propagator, it can be seen from Fig. 5 that the shape of the curves of the differential cross-sections of the  $t$ -distribution is relatively steep. This will be an important theoretical basis for us to clarify the role and contribution of the Regge propagator through EIC or UPCs experiments.

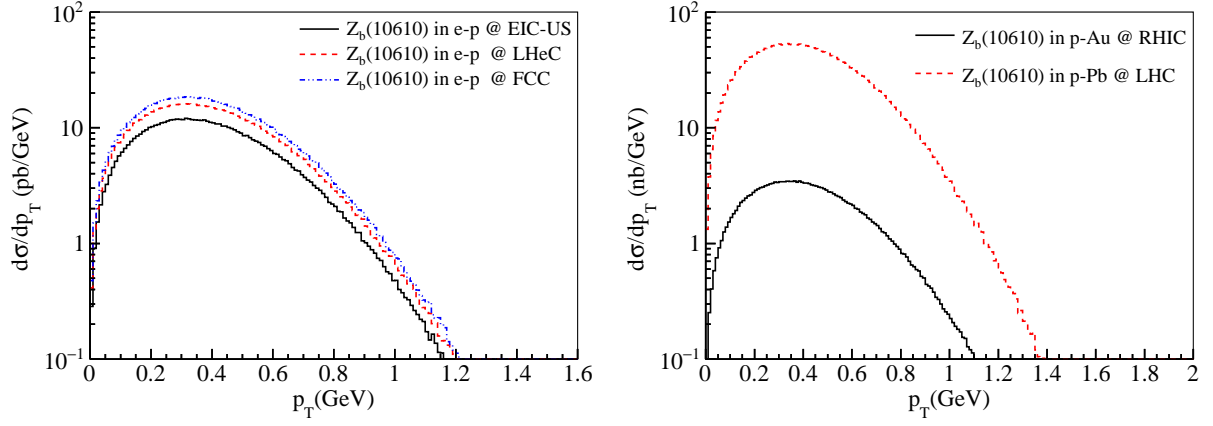


FIG. 4: (Color online) Transverse momentum distributions of  $Z_b(10610)$  in  $e-p$  at EIC-US, LHeC and FCC with  $0 < Q^2 < 1 \text{ GeV}^2$  and  $p\text{-Au}$  and  $p\text{-Pb}$  UPCs at RHIC and LHC.

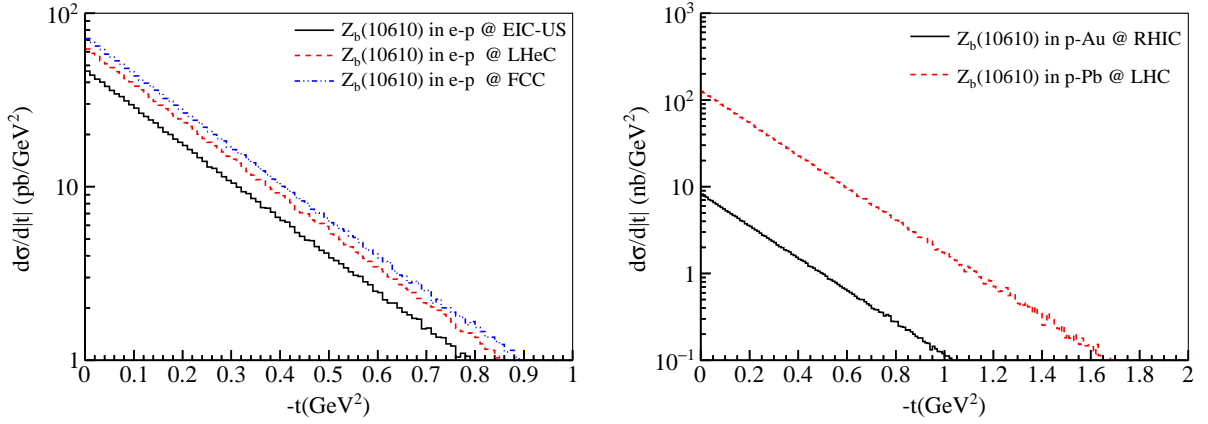


FIG. 5: (Color online) The  $t$ -distribution for the  $Z_b(10610)$  production in  $e-p$  and  $p\text{-A}$  scatterings.

#### IV. SUMMARY AND DISCUSSIONS

In this work, based on the effective field theory and the VMD mechanism, the photoproduction of two bottomonium-like  $Z_b(10610)$  and  $Z_b(10650)$  states are investigated for the first time. The numerical results show that the total cross-sections of the  $\gamma p \rightarrow Z_b n$  reaction reach a maximum at the center of mass energy  $W \simeq 22 \text{ GeV}$ , which indicates that the center of mass energy  $22 \text{ GeV}$  is the best energy window for searching for the  $Z_b$  states via  $\gamma p$  scattering. Hence, an experimental study of the bottomonium-like states  $Z_b$  via the  $\gamma p$  reaction is suggested.

With the help of eSTARlight and STARlight packages, the cross-sections and event numbers of  $Z_b(10610)$  production in EICs and UPCs have been presented in this work. As shown in Table II, the EICs may collect more events due to the larger luminosity. Moreover, we also simulated the rapidity and transverse momentum distributions of  $Z_b(10610)$  in  $e-p$  scattering and  $p\text{-A}$  UPCs processes. These results will provide an important basis for estimating the production and studying properties of  $Z_b$  in the RHIC, LHC, EIC-US, LHeC, and FCC in the future.

Since the Reggeons are composed mostly of quarks, using Reggeons to prove the distributions of sea quarks and anti-quarks in nuclei may be a feasible method [42]. In this work, the photoproduction of  $Z_b$  is calculated by introducing the Regge exchange model, thus, the numerical results will be beneficial for experimental studying of the Reggeon model. Also, the cross-section of  $t$  distribution of  $Z_b$  in different scattering processes are obtained, which will provide an important theoretical reference for clarifying the role and contribution of Reggeon.



## V. ACKNOWLEDGMENTS

This project is supported by the National Natural Science Foundation of China (Grant Nos. 12065014, 11705076 and 11747160), and by the Strategic Priority Research Program of Chinese Academy of Sciences, Grant No. XDB34030301. This work is partly supported by HongLiu Support Funds for Excellent Youth Talents of Lanzhou University of Technology. We also acknowledge the Natural Science Foundation of Fujian Province (Grant No. 2018J05007) and the Natural Science Foundation of Jimei University (Grant No. ZQ2017007).

- 
- [1] M. Tanabashi *et al.* [ParticleDataGroup], “Review of Particle Physics,” *Phys. Rev. D* **98**, 030001 (2018).
- [2] Y. R. Liu, H. X. Chen, W. Chen, X. Liu and S. L. Zhu, “Pentaquark and Tetraquark states,” *Prog. Part. Nucl. Phys.* **107**, 237-320 (2019).
- [3] F. K. Guo, X. H. Liu and S. Sakai, “Threshold cusps and triangle singularities in hadronic reactions,” *Prog. Part. Nucl. Phys.* **112**, 103757 (2020).
- [4] A. Bondar *et al.* (Belle Collaboration), *Phys. Rev. Lett.* **108**, 122001 (2012).
- [5] I. Adachi *et al.* (Belle Collaboration), arXiv:1105.4583; arXiv:1209.6450.
- [6] A. Garmash *et al.* (Belle Collaboration), *Phys. Rev. Lett.* **116**, 212001 (2016).
- [7] A. Garmash *et al.* (Belle Collaboration), *Phys. Rev. D* **88**, 052016 (2013).
- [8] A. Ali, C. Hambrook and W. Wang, *Phys. Rev. D* **85**, 054011 (2012). [arXiv:1110.1333 [hep-ph]].
- [9] A. Esposito, A. L. Guerrieri, F. Piccinini, A. Pilloni and A. D. Polosa, *Int. J. Mod. Phys. A* **30**, 1530002 (2015). [arXiv:1411.5997 [hep-ph]].
- [10] L. Maiani, A. Polosa and V. Riquer, *Phys. Lett. B* **778**, 247-251 (2018). [arXiv:1712.05296 [hep-ph]].
- [11] Z. G. Wang and T. Huang, *Nucl. Phys. A* **930**, 63-85 (2014).
- [12] A. Bondar, A. Garmash, A. Milstein, R. Mizuk and M. Voloshin, *Phys. Rev. D* **84**, 054010 (2011). [arXiv:1105.4473 [hep-ph]].
- [13] J. R. Zhang, M. Zhong and M. Q. Huang, *Phys. Lett. B* **704**, 312-315 (2011). [arXiv:1105.5472 [hep-ph]].
- [14] Z. F. Sun, J. He, X. Liu, Z. G. Luo and S. L. Zhu, *Phys. Rev. D* **84**, 054002 (2011). [arXiv:1106.2968 [hep-ph]].
- [15] H. W. Ke, X. Q. Li, Y. L. Shi, G. L. Wang and X. H. Yuan, *JHEP* **04**, 056 (2012). [arXiv:1202.2178 [hep-ph]].
- [16] J. Dias, F. Aceti and E. Oset, *Phys. Rev. D* **91**, 076001 (2015). [arXiv:1410.1785 [hep-ph]].
- [17] Q. Wang, V. Baru, A. Filin, C. Hanhart, A. Nefediev and J. L. Wintern, *Phys. Rev. D* **98**, 074023 (2018). [arXiv:1805.07453 [hep-ph]].
- [18] F. K. Guo, C. Hanhart, U. G. Meier, Q. Wang, Q. Zhao and B. S. Zou, *Rev. Mod. Phys.* **90**, 015004 (2018). [arXiv:1705.00141 [hep-ph]].
- [19] X. H. Liu, Q. Zhao and F. E. Close, “Search for tetraquark candidate  $Z(4430)$  in meson photoproduction,” *Phys. Rev. D* **77**, 094005 (2008).
- [20] J. He and X. Liu, “Discovery potential for charmonium-like state  $Y(3940)$  by the meson photoproduction,” *Phys. Rev. D* **80**, 114007 (2009).
- [21] G. Galata, “Photoproduction of  $Z(4430)$  through mesonic Regge trajectories exchange,” *Phys. Rev. C* **83**, 065203 (2011).
- [22] Q. Y. Lin, X. Liu and H. S. Xu, *Phys. Rev. D* **88**, 114009 (2013).
- [23] X. Y. Wang, X. R. Chen and A. Guskov, “Photoproduction of the charged charmoniumlike  $Z_c^+(4200)$ ,” *Phys. Rev. D* **92**, 094017 (2015).
- [24] X. Y. Wang, X. R. Chen and J. He, “Possibility to study pentaquark states  $P_c(4312)$ ,  $P_c(4440)$ , and  $P_c(4457)$  in  $\gamma p \rightarrow J/\psi p$  reaction,” *Phys. Rev. D* **99**, 114007 (2019).
- [25] X. Y. Wang, J. He and X. Chen, “Systematic study of the production of hidden-bottom pentaquarks via  $\gamma p$  and  $\pi^- p$  scatterings,” *Phys. Rev. D* **101**, 034032 (2020).
- [26] Y. P. Xie, X. Y. Wang and X. Chen, “Production of vector mesons in pentaquark states resonance channel in  $p$ - $A$  ultraperipheral collisions,” *Chin. Phys. C* **45**, 014107 (2021).
- [27] M. Albaladejo *et al.* [JPAC], “XYZ spectroscopy at electron-hadron facilities: Exclusive processes,” [arXiv:2008.01001 [hep-ph]].
- [28] T. H. Bauer, R. D. Spital, D. R. Yennie and F. M. Pipkin, “The Hadronic Properties of the Photon in High-Energy Interactions,” *Rev. Mod. Phys.* **50**, 261 (1978) Erratum: [*Rev. Mod. Phys.* **51**, 407 (1979)]. doi:10.1103/RevModPhys.50.261
- [29] T. Bauer and D. R. Yennie, “Corrections to VDM in the Photoproduction of Vector Mesons. 1. Mass Dependence of Amplitudes,” *Phys. Lett.* **60B**, 165 (1976).
- [30] T. Bauer and D. R. Yennie, “Corrections to Diagonal VDM in the Photoproduction of Vector Mesons. 2. Phi-omega Mixing,” *Phys. Lett.* **60B**, 169 (1976).
- [31] C. A. Bertulani, S. R. Klein and J. Nystrand, “Physics of ultra-peripheral nuclear collisions,” *Ann. Rev. Nucl. Part. Sci.* **55**, 271-310 (2005) [arXiv:nucl-ex/0502005 [nucl-ex]].
- [32] A. J. Baltz, G. Baur, d’Enterria, L. Frankfurt, F. Gelis, V. Guzey, K. Hencken, Y. Kharlov, M. Klasen, S. R. Klein, V. Nikulin, J. Nystrand, I. A. Pshenichnov, S. Sadovsky, E. Scapparone, J. Seger, M. Strikman, M. Tverskoy, R. Vogt, S. N. White, U. A. Wiedemann, P. Yepes and M. Zhalov, “The Physics of Ultraperipheral Collisions at the LHC,” *Phys. Rept.* **458**, 1-171 (2008) [arXiv:0706.3356 [nucl-ex]].
- [33] X. Chen, *PoS DIS* **2018**, 170 (2018) doi:10.22323/1.316.0170 [arXiv:1809.00448 [nucl-ex]].
- [34] C. Montag, Presented at the EIC Users Group Meeting 2017, Trieste, Italy, (2017).
- [35] J. L. Abelleira Fernandez *et al.* [LHeC Study Group], *J. Phys. G* **39**, 075001 (2012).
- [36] F. Bordry, M. Benedikt, O. Brning, J. Jowett, L. Rossi, D. Schulte, S. Stapnes and F. Zimmermann, [arXiv:1810.13022 [physics.acc-ph]].
- [37] S. R. Klein, J. Nystrand, J. Seger, Y. Gorbunov and J. Butterworth, “STARlight: A Monte Carlo simulation program for ultra-peripheral



- collisions of relativistic ions, *Comput. Phys. Commun.* **212**, 258-268 (2017).
- [38] M. Lomnitz and S. Klein, "Exclusive vector meson production at an electron-ion collider, *Phys. Rev. C* **99**, 015203 (2019).
- [39] G. Baur, K. Hencken, D. Trautmann, S. Sadovsky and Y. Kharlov, *Phys. Rept.* **364**, 359 (2002) [hep-ph/0112211].
- [40] X. Y. Wang, J. He, X. R. Chen, Q. Wang and X. Zhu, "Pion-induced production of hidden-charm pentaquarks  $P_c(4312)$ ,  $P_c(4440)$ , and  $P_c(4457)$ ," *Phys. Lett. B* **797**, 134862 (2019).
- [41] Z. W. Lin, C. M. Ko and B. Zhang, "Hadronic scattering of charm mesons," *Phys. Rev. C* **61**, 024904 (2000).
- [42] S. R. Klein and Y. P. Xie, "Photoproduction of charged final states in ultraperipheral collisions and electroproduction at an electron-ion collider," *Phys. Rev. C* **100**, 024620 (2019).
- [43] V. M. Budnev, I. F. Ginzburg, G. V. Meledin and V. G. Serbo, "The Two photon particle production mechanism. Physical problems. Applications. Equivalent photon approximation," *Phys. Rept.* **15**, 181 (1975).
- [44] O. Gryniuk, S. Joosten, Z. E. Meziani and M. Vanderhaeghen, [arXiv:2005.09293 [hep-ph]].
- [45] S. Klein and J. Nystrand, *Phys. Rev. C* **60**, 014903 (1999) [hep-ph/9902259].

